Rearrangement of Rhenium Allyl Vinyl Ketone Complexes

Charles P. Casey*, Todd L. Underiner, Paul C. Vosejpka, Greg A. Slough, James A. Gavney, Jr., and Randy K. Hayashi

Department of Chemistry, University of Wisconsin, Madison, Wisconsin 53706

Received January 3, 1997[⊗]

The isomerization of parallel−perpendicular allyl vinyl ketone complex $C_5H_5(CO)Re(\eta^2,\eta^2$-$H_2C{=}CHCH_2COCH{=}CHCH_2CMe_3)$ (**2**) to the diastereomeric perpendicular−parallel complex $C_5H_5(CO)Re(\eta^2,\eta^2$-$H_2C{=}CHCH_2COCH{=}CHCH_2CMe_3)$ (**6**) occurred without formation of an unsaturated intermediate trappable by either PMe_3 or ^{13}CO. The rearrangement of *exo*-$C_5H_5(CO)Re[\eta^2,\eta^2$-$CH_2{=}CHCH(CH_3)COCH{=}CHCH_2CMe_3]$ (**8-exo**) occurred with retention of stereochemistry at rhenium and with enantioface inversion of both complexed alkenes. The kinetically formed parallel−perpendicular isomer **8**-exo rearranged by sequential enantioface inversion of the vinyl π-bond to give parallel−parallel intermediate *exo*-C_5H_5-$(CO)Re[\eta^2,\eta^2$-$CH_2{=}CHCH(CH_3)COCH{=}CHCH_2CMe_3]$ (**12-exo**) and then enantioface inversion of the allyl π-bond to form the perpendicular−parallel isomer *exo*-$C_5H_5(CO)Re[\eta^2,\eta^2$-$CH_2{=}CHCH(CH_3)COCH{=}CHCH_2CMe_3]$ (**9-exo**). Enolization of allyl vinyl ketone complexes was observed, but is not required for the isomerization. C−H insertion mechanisms involving a net hydrogen migration were excluded by deuterium labeling studies. A mechanism in which rhenium migrates to the opposite enantiofaces of the alkene ligands via σ-C−H complexes is proposed.

Introduction

We recently reported the unusually facile rearrangement of the allyl vinyl rhenium complex $C_5H_5(CO)_2Re$-$(CH_2CH{=}CH_2)((E)$-$CH{=}CHCH_2CMe_3)$ (**1**) to the allyl vinyl ketone complex $C_5H_5(CO)Re(\eta^2,\eta^2$-$H_2C{=}CHCH_2$-$COCH{=}CHCH_2CMe_3)$ (**2**).[1,2] In contrast, the methyl vinyl rhenium complex *trans*-$C_5H_5(CO)_2Re(CH_3)((E)$-$CH{=}CHCH_2CMe_3)$ (**3**) was stable for hours at 90 °C. A key to understanding the mechanism of formation of **2** was the observation that the isopropyl allyl rhenium complex *trans*-$C_5H_5(CO)_2Re(CH_2CH{=}CH_2)(CHMe_2)$ (**4**) rearranged to the stable η^3-allyl acyl complex $C_5H_5(CO)$-$Re(exo$-η^3-$CH_2CHCH_2)(COCHMe_2)$ (**5**), which did not undergo reductive elimination to give a ketone. A second important observation came from a deuterium labeling study, which showed that $C_5H_5(CO)_2Re(CD_2$-$CH{=}CH_2)((E)$-$CH{=}CHCH_2CMe_3)$ (**1**-d_2), with deuterium label on the sp^3 allyl carbon rearranged to $C_5H_5(CO)$-$Re(\eta^2,\eta^2$-$D_2C{=}CHCH_2COCH{=}CHCH_2CMe_3)$ (**2**-d_2), which had deuterium on the sp^2 allyl carbon. A third important observation was that X-ray crystallographic analysis showed that the allyl vinyl ketone complex **2** had an interesting geometry in which the alkene ligands are "crossed" (Table 1). The double bond of the allyl ligand was roughly parallel to the plane of the cyclopentadienyl ligand, while the vinyl ligand was coordinated roughly perpendicular to that plane.[3]

We proposed that the conversion of **1** to **2** occurs by two consecutive concerted organometallic rearrangements.[1,2] In each of these rearrangements, two steps are combined to avoid the generation of a high-energy coordinatively unsaturated intermediate; one of the steps would normally generate a vacant coordination site while the other would consume a vacant coordination site. In the first concerted reaction, the migration of a vinyl group to CO is assisted by conversion of a σ-allyl to a π-allyl group. Such an assisted migration is not possible for the very thermally stable methyl vinyl complex **3**. In the second concerted reaction, the reductive elimination of the allyl and acyl groups is assisted by coordination of the vinyl double bond. Vinyl coordination is readily achieved only from the s-trans conformation of the unsaturated acyl group; this explains the unusual parallel−perpendicular coordination of the double bonds of allyl vinyl ketone complex **2**. Such an assisted reductive elimination is not possible for the isopropyl-substituted acyl allyl complex **5**.

To determine whether the unusual parallel−perpendicular geometry of **2** was kinetically or thermodynamically controlled, **2** was heated to 100 °C for 3 weeks. Equilibration with a second allyl vinyl ketone diastereomer $C_5H_5(CO)Re(\eta^2,\eta^2$-$H_2C{=}CHCH_2COCH{=}CHCH_2$-$CMe_3)$ (**6**) (**2**:**6** ≈ 1:2) occurred.[2] The crystal structure of **6** showed that the allyl and vinyl ligands were again coordinated in a "crossed" fashion; however, in **6**, the *vinyl* ligand is coordinated roughly parallel to the plane of the cyclopentadienyl ligand, while the *allyl* ligand is coordinated perpendicular to that plane (Scheme 1). During the isomerization, a third compound with a Cp resonance at δ 5.18 grew to ~8% of the mixture and then decreased to a steady state of ~4%. The possibility that this third compound might be the parallel−parallel

[⊗] Abstract published in *Advance ACS Abstracts,* April 15, 1997.

(1) Casey, C. P.; Vosejpka, P. C.; Gavney, Jr., J. A. *J. Am. Chem. Soc.* **1990**, *112,* 4083.

(2) Casey, C. P.; Vosejpka, P. C.; Underiner, T. L.; Slough, G. A.; Gavney, J. A., Jr. *J. Am. Chem. Soc.* **1993**, *115,* 6680−6688.

(3) To more quantitatively discuss the geometry of $Cp(CO)_2Re$-(alkene) complexes, we focus attention on the angle between the plane defined by the Cp centroid, Re, and the center of the alkene C=C bond and the plane defined by Re and the C=C bond. We will refer to two extreme geometries: a parallel geometry (90° interplanar angle) and a perpendicular geometry (0° interplanar angle).

S0276-7333(97)00004-6 CCC: $14.00

Table 1. Selected Bond Lengths (Å) and Angles (deg) for Allyl Vinyl Ketone Complexes[a]

	2	6	8-exo	8-endo	9-exo	12-exo
Re−C(1)	2.196(21)	2.186(12)	2.23(2)	2.21(2)	2.201(4)	2.225(4)
Re−C(2)	2.246(19)	2.295(12)	2.25(2)	2.220(14)	2.300(4)	2.223(3)
Re−C(5)	2.243(15)	2.199(8)	2.27(2)	2.291(14)	2.201(4)	2.224(3)
Re−C(6)	2.188(17)	2.226(8)	2.17(2)	2.178(13)	2.199(4)	2.267(3)
C(1)−C(2)	1.417(29)	1.411(15)	1.40(3)	1.41(2)	1.408(7)	1.412(5)
C(5)−C(6)	1.416(21)	1.445(12)	1.39(2)	1.44(2)	1.436(6)	1.411(5)
C(1)−C(2)−C(3)	120.8(18)	121.3(9)	115(2)	120(2)	120.9(4)	125.5(3)
C(4)−C(5)−C(6)	121.7(15)	122.6(8)	122(2)	123.9(13)	123.5(4)	121.9(3)
C(5)−C(6)−C(7)	119.2(12)	119.1(7)	119.4(13)	119.5(13)	119.4(4)	120.7(3)
allyl interplanar	82.5	10.2	73.8	79.1	9.9	76.0
vinyl interplanar	8.6	82.1	1.2	4.7	80.3	80.8

[a] The allyl and the vinyl interplanar angles are the angles between the plane defined by the Cp centroid, Re, and the center of the alkene C═C bond and the plane defined by Re and the C═C bond.

Scheme 1

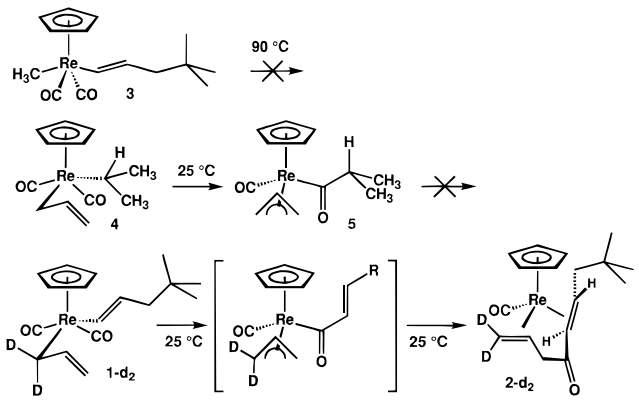

diastereomer $C_5H_5(CO)Re(\eta^2,\eta^2\text{-}H_2C{=}CHCH_2COCH{=}CHCH_2CMe_3)$ (**7**) was considered, but it was not possible to isolate or fully characterize this compound. Another possible structure for the third compound would be the perpendicular−perpendicular diastereomer **A**.

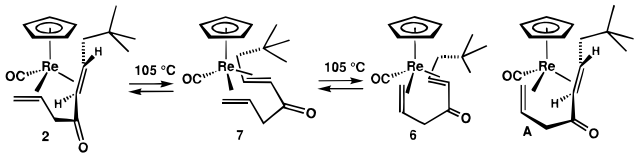

Here we report detailed mechanistic studies of this isomerization process that exclude a number of plausible mechanisms. We suggest that the isomerization of **2** to **6** occurs by migration of Re from one enantioface of the vinyl double bond to the other to produce the parallel−parallel diastereomer **7**; this is suggested to occur via an intermediate in which a vinyl C−H bond is agostically linked to Re. In a second step, Re is suggested to migrate from one enantioface of the allyl double bond to the other again via an intermediate with an agostic C−H−Re interaction.

Results and Discussion

Rather than detail all of the plausible mechanisms from the start, we will introduce mechanistic possibilities for rearrangement of allyl vinyl ketone complexes in the context of experiments designed to distinguish between mechanisms.

Stereochemistry of Allyl Vinyl Ketone Complexes. In analyzing the interconversion of the diastereomeric allyl vinyl ketone rhenium complexes **2** and **6**, it is important to note that there are essentially three stereocenters in compounds **2** and **6**: the Re center, the

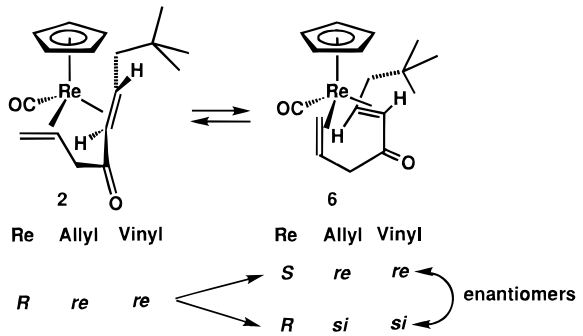

allyl π-face, and the vinyl π-face.[4] The *R, re, re* enantiomer of **2** can be converted to **6** either by inversion at rhenium to produce the *S, re, re* enantiomer of **6** or by inversion at both alkene enantiofaces to produce the *R, si, si* enantiomer of **6**. Since **2** was necessarily formed as a racemic mixture, it was not possible to distinguish between rhenium inversion and alkene inversion.

Dissociative Mechanisms. Two different dissociative mechanisms for conversion of **2** to **6** were considered. First, dissociation of CO from **2**, followed by readdition of CO to the opposite side of Re produces **6** without the intervention of the parallel−parallel complex **7**. This process inverts the stereochemistry of the Re center but maintains the stereochemistry of the allyl and vinyl enantiofaces. Second, dissociation of one coordinated alkene from **2**, followed by addition of rhenium to the opposite alkene enantioface, would produce a new diene complex (**7** or possibly **A**) which could then dissociate the other alkene and add rhenium to its opposite alkene enantioface. This process produces **6** with retention of stereochemistry at the Re center but inversion of the allyl and vinyl enantiofaces.

Isomerization without the Intervention of a Trappable Intermediate. To test for dissociative mechanisms, the equilibration of **6** and **2** was carried out under an atmosphere of ^{13}CO. A CD_3CN solution of **6** was sealed in an NMR tube under 0.8 atm of ^{13}CO. ^{13}C NMR spectroscopy revealed no incorporation of ^{13}CO into the carbonyl resonances of **6** or **2** even after 5 weeks (>50 half-lives) at 100 °C. In a second attempt to trap an intermediate, a CD_3CN solution of **2** containing 2 equiv of PMe_3 was heated at 85 °C in an NMR tube. No formation of species containing a PMe_3 ligand was observed by ^1H NMR spectroscopy. Qualitatively, the

(4) Each carbon of the vinyl ligand is a stereocenter. However, as long as cis−trans isomerization of the vinyl carbon−carbon double bond does not occur, the two stereocenters will always change in tandem. We therefore treat them as one stereocenter given by the face (*re* or *si*) of the double bond coordinated to rhenium.

Scheme 2

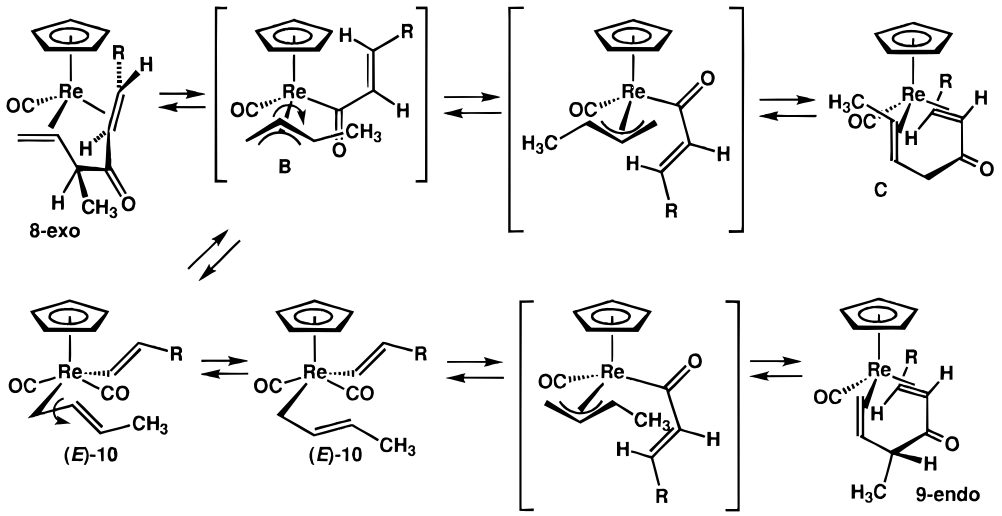

rate of isomerization to **6** was not significantly different from the thermolysis of **2** in the absence of PMe_3.

Mechanisms Involving Reversible Formation of π-Allyl or σ-Allyl Intermediates. Two possible mechanisms for interconversion of allyl vinyl ketone complexes **2** and **6** involve reversal of the carbon−carbon bond forming processes involved in the formation of **2** from σ-allyl vinyl complex **1**. The first involves reversal to a π-allyl acyl complex, rotation of the π-allyl unit, and reformation of the carbon−carbon bond. Depending on how the vinyl group recomplexes to rhenium, this mechanism could either produce **6** directly or could form the parallel−parallel isomer **7** as an intermediate. The second process begins with the same reversal to a π-allyl acyl complex and proceeds back to the starting σ-allyl vinyl complex **1**, which can then re-form carbon−carbon bonds and produce **2**, **6**, or **7**.

To test these mechanistic possibilities, we set out to synthesize *exo*-$C_5H_5(CO)Re[\eta^2,\eta^2$-$CH_2{=}CHCH(CH_3)$-$COCH{=}CHCH_2CMe_3]$ (**8-exo**), which has an additional stereocenter on the allyl side chain. This additional stereocenter makes it possible to determine stereochemical changes at Re and at the alkene enantiofaces occurring in the interconversion of allyl vinyl ketone isomers. Isomerization of parallel−perpendicular **8-exo** to a perpendicular−parallel allyl vinyl ketone complex via the π-allyl acyl intermediate **B** requires rotation of the π-allyl unit and will result in an easily detected net methyl migration to give complex **C** (Scheme 2). Isomerization of **8-exo** via reversal to the σ-allyl vinyl complex (***E*)-10** would lead to formation of perpendicular−parallel isomer **9-endo**.

Note that the stereochemistry of the rearrangement of **8**-exo also provides an additional sensitive test for the CO dissociation mechanism. Even if CO never leaves the solvent cage and cannot exchange with external ^{13}CO, the CO dissociation mechanism predicts the formation of **9-endo**. Intramolecular rearrangement of **8-exo** via an admittedly unlikely pivot mechanism would also lead to the formation of **9-endo**.

If it proved impossible to obtain X-ray structures, we anticipated that we would be able to determine the stereochemistry at the methyl-substituted allylic carbons of **8-exo**, **8-endo**, **9-exo**, and **9-endo** from the magnitude of the allylic vicinal ($^3J_{=CHCH\mathrm{MeCO}}$) coupling constant in the ^1H NMR spectra. For the unsubstituted

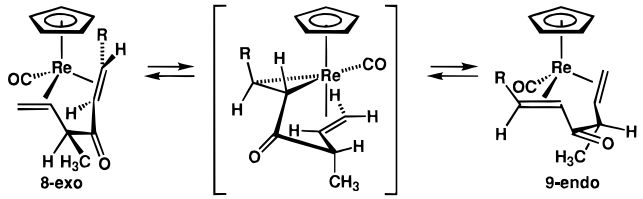

parallel−perpendicular allyl vinyl ketone complex **2**, only the allylic proton at δ 2.00 (dd, J = 16.3, 6.3 Hz) showed significant coupling to the adjacent vinyl proton at δ 2.10 (m), while the other allylic proton at δ 1.66 (d, J = 16.3 Hz) had <1 Hz coupling to the same proton. In the X-ray structure of **2**, the dihedral angles between the allylic hydrogens and the adjacent vinyl hydrogen were −48.5 (exo proton) and +72.5° (endo proton). Based on the expected angular dependence of coupling constants,[5] the large 6.3 Hz coupling can be confidently assigned to the exo proton with a −48.5° dihedral angle while the negligible <1 Hz coupling is assigned to the endo proton with a +72.5° dihedral angle. This predicts that the related coupling for **8-exo** should be substantially smaller than the coupling in **8-endo** (Scheme 3). Similarly, in the X-ray crystal structure of the unsubstituted perpendicular−parallel allyl vinyl ketone complex **6**, the dihedral angles between the allylic hydrogens and the adjacent vinyl hydrogen were −75.5° (exo proton) and +44.8° (endo proton). In the ^1H NMR of **6**, one allylic proton at δ 2.06 (J = 15.2 Hz, 6.4 Hz) showed a large coupling to the adjacent C*H*=C proton, while the other allylic proton at δ 1.99 (J = 15.2 Hz, <1 Hz) displayed negligible coupling. The large 6.4 Hz coupling was confidently assigned to the endo proton with a +44.8° dihedral angle, while the <1 Hz coupling constant is assigned to the exo proton with a −75.5° dihedral angle. This predicts that the related coupling for **9-exo** should be substantially larger than the coupling in **9-endo** (Scheme 3).

Synthesis of α-Methyl Derivatives 8-exo and 8-endo. When a CH_3CN solution of the rhenium vinyl anion complex $K^+Cp(CO)_2Re[(E)$-$CH{=}CHCH_2CMe_3]^-$ (**11**) was treated with excess 1-bromo-2-butene (crotyl

(5) (a) Silverstein, R. M.; Bassler, G. C.; Morrill, T. C. *Spectrometric Identification of Organic Compounds*, 4th ed.; John Wiley & Sons: New York, 1981. (b) Gordon, A. J.; Ford, R. A. *The Chemist's Companion*; John Wiley & Sons: New York, 1972.

Scheme 3

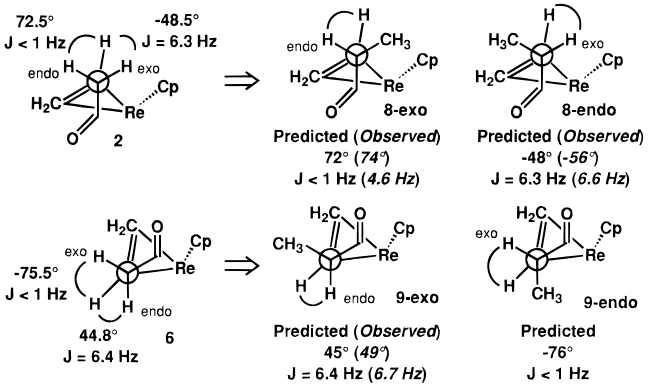

bromide, predominantly trans isomer) for 4 h, formation of a 2.7:1 ratio of two new allyl vinyl ketone complexes *exo*-Cp(CO)Re[η^2,η^2-CH_2=CHCH(CH_3)COCH=$CHCH_2$-CMe_3] (**8-exo**) and *endo*-Cp(CO)Re[η^2,η^2-CH_2=CHCH-(CH_3)COCH=$CHCH_2CMe_3$] (**8-endo**) was observed by ^{1}H NMR spectroscopy (Scheme 4). These diastereomers, which are epimers at the methyl-substituted carbon α to the ketone carbonyl, were separated by preparative thin-layer chromatography.

Scheme 4

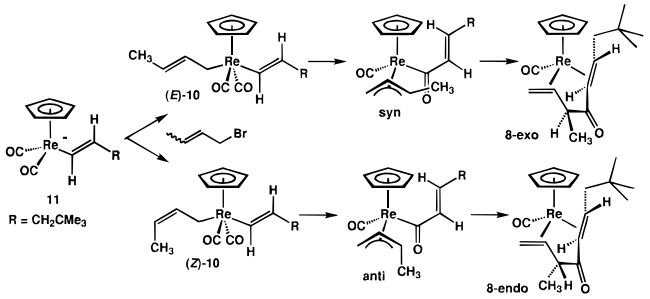

The formation of **8-exo** and **8-endo** is readily interpreted in terms of the detailed mechanism for the formation of **2** from allyl vinyl rhenium complex **1**. The (*E*)-2-butenyl vinyl rhenium isomer (*E*)-**10**, formed from alkylation of **11** with *trans*-crotyl bromide, would be expected to rearrange to a syn π-allyl acyl intermediate prior to coupling of the allyl and acyl ligands. This leads to an allyl vinyl ketone complex (**8-exo**) with the methyl group in the exo position α to the ketone carbonyl. The (*Z*)-2-butenyl vinyl rhenium isomer (*Z*)-**10**, formed by alkylation of **11** with the minor *cis*-crotyl bromide present in solution, would be expected to rearrange to an anti π-allyl intermediate prior to coupling of the allyl and acyl ligands. This leads to an allyl vinyl ketone complex (**8-endo**) with the methyl group in the endo position α to the ketone carbonyl.

In the crystal structure of **8-exo** (Figure 1, Table 1), the allylic double bond is roughly parallel to the plane of the Cp ligand (73.8° interplanar angle[3]). The vinyl double bond roughly bisects the Cp plane (1.2° interplanar angle[3]). The α-methyl group is clearly in the exo position relative to the Cp ring, with a dihedral angle of +73.8° between the α-allylic proton and the adjacent vinyl proton.

It is fortunate that we obtained an X-ray crystal structure of **8-exo** since assignment of stereochemistry from the magnitude of the allylic vicinal ($^3J_{=CHCH\text{MeCO}}$) coupling constant would have been problematic. While

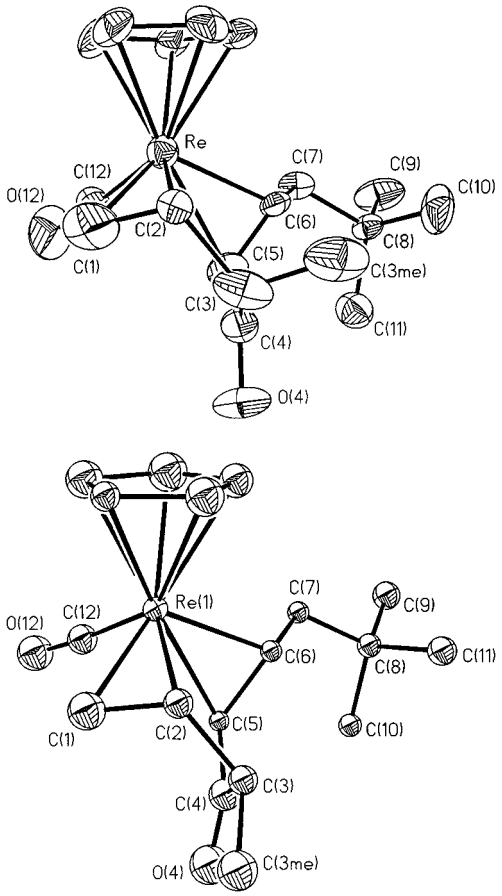

Figure 1. X-ray crystal structures of **8-exo** (top) and **8-endo** (bottom).

the 4.6 Hz magnitude of this coupling was smaller than the 6.6 Hz coupling seen for the **8-endo** isomer (see below) as predicted, its absolute value was substantially larger than the <1 Hz coupling observed for **2** even though the dihedral angle differed by only 1.3°.

In the X-ray crystal structure of **8-endo** (Figure 1, Table 1) the allylic double bond is roughly parallel to the cyclopentadienyl ring (79.1° interplanar angle[3]) and the vinyl double bond is roughly perpendicular to the cyclopentadienyl ring (4.7°) interplanar angle[3]). The dihedral angle between the α-allylic proton and the adjacent vinyl proton was −55.8°, 7.3° greater than the dihedral angle between the exo allylic proton and the adjacent vinyl proton of **2**. A 6.6 Hz coupling was observed between these two protons in the ^{1}H NMR spectrum of **8-endo**. The greater magnitude of this coupling for **8-endo** compared with **8-exo** is consistent with predictions based on the X-ray structures and NMR spectra of **2** and **6**.

Equilibration of 8-exo with parallel−parallel Isomer 12-exo and perpendicular−parallel Isomer 9-exo. A CD_3CN solution of **8-exo** was heated in an oil bath at 99.8 °C and periodically monitored by ^{1}H NMR spectroscopy. After 1 h, a mixture of 71% **8-exo**, 27% of the parallel−parallel isomer Cp(CO)Re(η^2,η^2-CH_2=CHCHCH_3COCH=$CHCH_2CMe_3$) (**12-exo**) (Cp δ 5.21; see below), and 2% of the perpendicular−perpendicular isomer Cp(CO)Re(η^2,η^2-CH_2=CHCHCH_3COCH=$CHCH_2CMe_3$) (**9-exo**) (Cp δ 5.10; see below) was observed. After 3 h, the mixture consisted of 49% **8-exo**, 44% **12-exo**,and 7% **9-exo**. At long times, an equilibrium mixture of 8% **8-exo**, 10% **12-exo**, and 82% **9-exo**

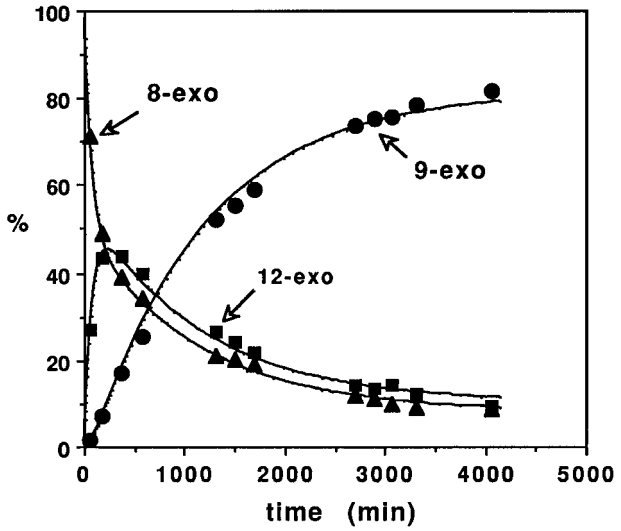

Figure 2. Isomerization of **8-exo** to **9-exo** in CD_3CN at 99.8 °C.

was observed. On longer heating, a trace of **8-endo** was formed. The data were fit to a kinetic model using the program GEAR[6] with $k_{8\rightarrow12} = (1.20 \pm 0.02) \times 10^{-4}$ s^{-1}, $k_{12\rightarrow8} = (9.5 \pm 0.1) \times 10^{-5}$ s^{-1}, $k_{12\rightarrow9} = (2.23 \pm 0.04) \times 10^{-5}$ s^{-1}, and $k_{9\rightarrow12} = (2.8 \pm 0.1) \times 10^{-6}$ s^{-1}. Figure 2 illustrates how well the experimental points fall on the lines calculated from this kinetic model.

When the thermolysis of **8**-exo was carried out for 5 days, ^{1}H NMR analysis showed a mixture of 8% **8-exo** (δ 5.03), 10% **12-exo** (δ 5.21), 72% **9-exo** (δ 5.10), and

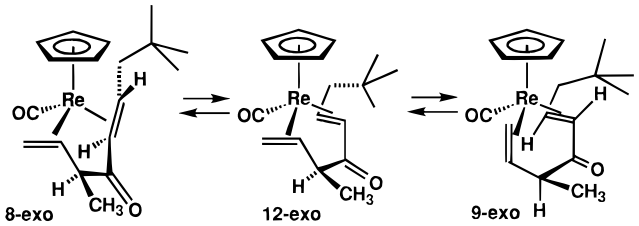

two minor Cp resonances at δ 5.14 (5%) and 4.98 (5%). Pure **9-exo** was isolated in 44% yield from preparative TLC followed by recrystallization from cold CH_3CN. The initial stereochemical assignment of the methyl group to the exo position of **9-exo** was based on analysis of the $^3J_{HH}$ coupling between the allylic proton α to the carbonyl group and the adjacent vinyl proton. The α-proton resonance was a pentet (J = 6.7 Hz) at δ 1.96. The pentet results from accidental equivalence of the couplings of the α-proton to the α-methyl group and to the adjacent vinyl proton. The large, 6.7 Hz coupling between the α-proton and the adjacent vinyl proton is similar to the 6.4 Hz coupling observed between the endo proton of **6** and the central allylic proton. A smaller coupling (<1 Hz) would have been expected if the methyl group were endo.

X-ray crystallographic analysis confirmed the assignment of the stereochemistry of **9-exo** (Figure 3, Table 1). The coordination geometry of **9-exo** is very similar to that of the rearranged perpendicular−parallel allyl vinyl ketone diastereomer **6**. The allylic double bond

(6) Weigert, F. J.; McKinney, R. J. GEAR PC3003, Project SERAPHIM, Department of Chemistry, University of Wisconsin−Madison, Madison WI 53706, 1991.

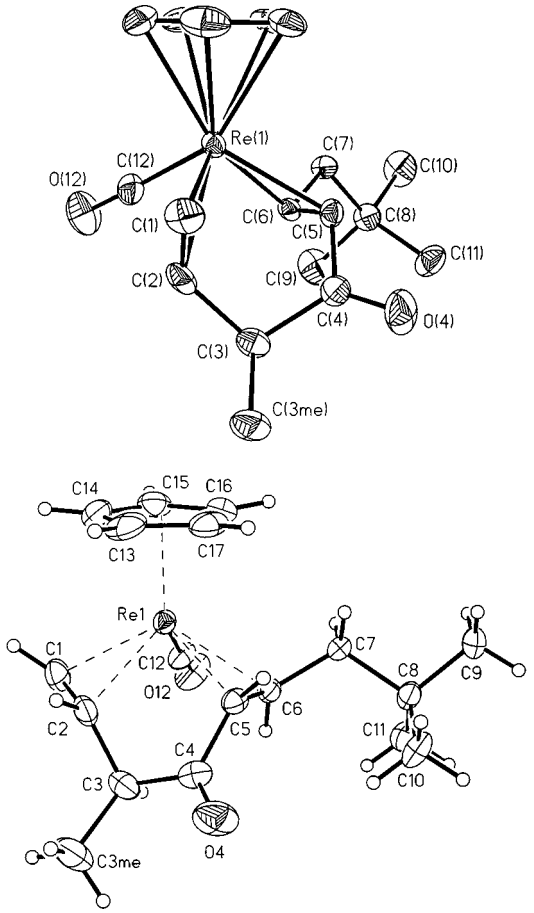

Figure 3. X-ray structures of **9**-exo (top) and **12**-exo (bottom).

is coordinated to rhenium in a plane roughly perpendicular to the cyclopentadienyl ring (−9.9° interplanar angle[3]). The vinyl double bond is roughly parallel to the cyclopentadienyl ring (80.3° interplanar angle[3]). The dihedral angle between the allylic proton and the adjacent proton was 49.0°. This is consistent with the observed large ^{1}H NMR coupling constant between these protons.

When the thermolysis of **8-exo** was carried out for 2 h, ^{1}H NMR analysis showed a 1.2:1 ratio of Cp resonances for starting material **8-exo** (δ 5.03)/**12-exo** (δ 5.21), and a small amount of **9-exo** (δ 5.10). Pure **12-exo** was isolated from a faster moving yellow band on preparative TLC. Single crystals of **12-exo** were obtained by cooling a concentrated CD_3CN solution of **9**-exo to −20 °C.

X-ray crystallographic analysis established the structure of **12-exo** as a parallel−parallel allyl vinyl ketone isomer with an allylic *exo*-methyl group (Figure 3, Table 1). Both the allylic double bond (76.0° interplanar angle[3]) and the vinyl double bond (80.8° interplanar angle[3]) are coordinated to rhenium in a plane roughly parallel to the cyclopentadienyl ring. The dihedral angle between the allylic proton at C(3) and the adjacent vinyl proton at C(2) was 170.1°. This is consistent with the observed large ^{1}H NMR coupling constant between these protons.

In the ^{1}H NMR spectrum of **12-exo**, the β-proton of the enone fragment of this parallel−parallel isomer appeared at δ 2.29 (ddd, J = 11.6, 9.5, 2.3 Hz), shifted

to much lower frequency than for the parallel−perpendicular and perpendicular−parallel allyl vinyl ketone isomers [δ 2.9−4.0, ddd, typical J = 11, 9, 2 Hz]. The α-proton of the enone ligand of **12-exo** was shifted to much *higher* frequency (δ 4.29, d, J = 9.6 Hz) than was observed for other isomers. The allylic proton α to the carbonyl of **12-exo** displayed a large 9.5 Hz coupling to the adjacent vinyl proton. This large coupling constant is consistent with the anti relationship (170.1° dihedral angle) of the central allylic proton and the allylic proton α- to the carbonyl.

Thermolysis of 8-endo occurred much more slowly than that of **8-exo**. ^{1}H NMR analysis of a CD_3CN solution of **8-endo** heated at 100 °C for 13 days revealed a 25% loss of starting material and formation of new Cp resonances at δ 5.15 (5%), 5.14 (10%), and 5.10 (10%, **9-exo**). Due to the small quantities of new complexes formed, no attempt was made to isolate any rearranged products.

Mechanistic Interpretation of the Isomerization of 8-exo. The observation that **8-exo** rearranged cleanly to **9-exo** establishes that stereochemistry at Re is maintained and that both alkenes have undergone enantioface inversion. This observation rules out mechanisms that involve reversion of the carbon−carbon bond forming processes to π-allyl acyl intermediate **B** (which would have produced methyl migration product **C**) or σ-allyl vinyl intermediate **10** (which would have given **9-endo**) (Scheme 2). The formation of **9-exo** is also inconsistent with the CO dissociation and pivot mechanisms described earlier. Only mechanisms in which the alkene π-bonds dissociate from rhenium and then coordinate through their opposite enantiofaces can explain the formation of **9-exo**. Exactly how the metal gets from one alkene enantioface to the other without the intervention of a trappable coordinatively unsaturated intermediate is a dilemma.

The observation that **8-exo** rearranges first to the parallel−parallel allyl vinyl ketone complex **12-exo** and then to **9-exo** establishes a sequence in which rhenium first migrates to the opposite enantioface of the vinyl double bond and then migrates to the opposite enantioface of the allyl double bond.

Exclusion of Enol Intermediates. Enols might play two important roles in the isomerization chemistry of allyl vinyl ketone complexes. First, they might mask intrinsic stereochemical information. For example, if **8-exo** rearranged directly to **9-endo**, which then rapidly isomerized via an enol intermediate to **9-exo**, then the observed formation of **9-exo** would provide no meaningful mechanistic information.

Second, enol intermediates could provide a pathway for isomerization not involving coordinatively unsaturated intermediates. Enolization followed by migration of rhenium from the vinyl double bond to the enol double bond could produce diene complex **D**. The uncomplexed vinyl double bond of **D** could rotate and rhenium could migrate to the opposite alkene enantioface (Scheme 5).

Enol formation should lead to H−D exchange with CD_3OD. When a solution of the unsubstituted allyl vinyl ketone complex **2** in 4:1 CD_3CN/CD_3OD was monitored by ^{1}H NMR, no H−D exchange into any position of **2** was observed on standing at room temperature for 2 weeks. Upon heating at 105 °C for 1 week,

Scheme 5

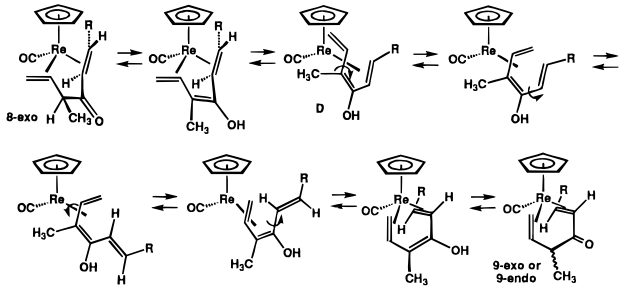

formation of a 1:1.1 ratio of **2/6** was observed. Separation of the isomers by preparative TLC aided ^{1}H NMR analysis, which showed nearly complete deuteration of the allylic protons of both **6** and **2**.

These observations indicate that enol formation occurs under the conditions of isomerization of **2** to **6** and suggested that the rearranged product **9-exo** formed from thermolysis of **8-exo** may have been produced by a *thermodynamic* protonation of the enol form of **9-exo**. However, the possibility that enol formation is required in the isomerization of **8-exo** to **9-exo** was ruled out by the observation that **8-exo** isomerized to **9-exo** in the presence of CD_3OD with <2% incorporation of deuterium α- to the carbonyl, as determined by ^{1}H NMR spectroscopy. Similarly, no H−D exchange was observed when the methyl isomer **8-endo** was heated at 100 °C in the presence of CD_3OD. Apparently, enol formation is much slower for the sterically more demanding α-methyl allyl vinyl ketone derivatives than for the parent allyl vinyl ketone complexes **2** and **6**.

Further evidence that enol formation is not required for the alkene enantioface inversion of allyl vinyl ketone complexes was obtained from observation of the isomerization of the α,α-dimethyl derivative Cp(CO)Re[η^2,η^2-CH_2=CHC$(CH_3)_2$COCH=CHCH_2CMe_3] (**13**), which has no acidic protons α- to the ketone carbonyl and cannot form an enol intermediate. **13** was prepared in high yield by reaction of $K^+C_5H_5(CO)_2$Re[(*E*)-CH=CHCH_2-CMe_3]$^-$ (**11**) with excess 4-bromo-2-methyl-2-butene. Thermolysis of **13** for 3 h at 100 °C led to initial conversion to a mixture of 72% starting material **13** and 28% of the parallel−parallel isomer **14**, which was characterized spectroscopically. After 180 h, an equi-

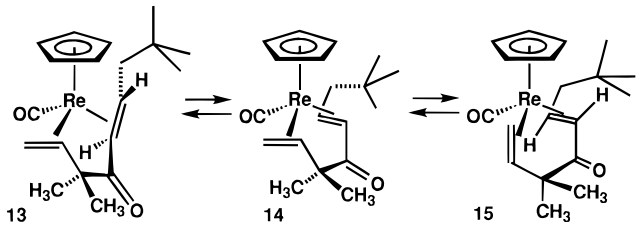

librium mixture of 50% **13**, 28% **14**, and 22% perpendicular−parallel isomer **15** was observed.

Exclusion of Hydrogen Transfer between Vinyl and Allyl Groups. In related studies of the rearrangement of a propargyl vinyl rhenium complex to an allenyl vinyl ketone complex, we discovered that the rhenium allenyl vinyl ketone complex Cp(CO)Re(η^2,η^2-CH_2=C=CHCOCH=CHCH_2CMe_3) (**16**) stereospecifically transferred a hydrogen from the β-vinyl position of the enone ligand to the central carbon of the η^2-allene ligand to

Scheme 6

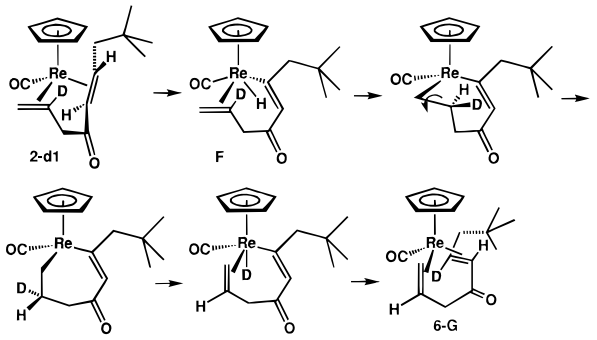

produce an η^3-allyl vinyl ketone complex Cp(CO)Re(η^3-$CH_2CHCHCOCH{=}CCH_2CMe_3$) (**17**).[7] One mechanism

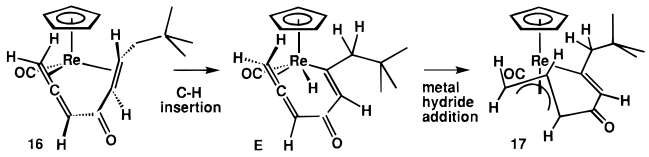

considered for this transformation involves insertion of rhenium into the β-C−H bond to produce intermediate **E**, which contains metal hydride, σ-vinyl, and η^2-allene ligands. Addition of this metal hydride to the η^2-allene ligand could produce the observed π-allyl ligand.

A related C−H insertion mechanism for the isomerization of **2** to **6** predicts hydrogen migration between the allyl and vinyl groups that can be tested by studying the isomerization of the deuterated analog **2**-d_1 (Scheme 6). Insertion of rhenium into a β-vinyl C−H bond of **2**-d_1 would produce an intermediate **F** which contains hydride, σ-vinyl, and η^2-alkene ligands. Addition of the metal hydride of **F** to the η^2-alkene would produce a σ-alkyl ligand, which could rotate about the former carbon−carbon double bond and eliminate a β-deuterium to produce an η^2-alkene ligand perpendicular to the Cp group. Reductive elimination of the rhenium deuteride and the σ-vinyl group restores an allyl vinyl ketone complex and places deuterium on the vinyl group. Depending on the geometry of the reductive elimination, the vinyl double bond could coordinate to rhenium in a plane parallel to the Cp ring to give **6-G** or perpendicular to the Cp ring to give a deuterated perpendicular−perpendicular isomer **A**.

To test this proposed mechanism, deuterium-labeled allyl vinyl ketone complex **2**-d_1 was prepared from $K^+C_5H_5(CO)_2Re[(E)\text{-}CH{=}CHCH_2CMe_3]^-$ (**11**) and $CH_2{=}CDCH_2Br$.[8] The mechanism shown in Scheme 6 predicts deuterium migration from the allyl fragment to the vinyl fragment. However, rearrangement of **2**-d_1 produced **6**-d_1 in which all the deuterium remained on the allyl fragment. This observation rigorously excludes the C−H insertion mechanism shown in Scheme 6. However, C−H insertion mechanisms that proceed by formation of intermediate **F** followed by reductive elimination of the rhenium hydride and the σ-vinyl group to form the parallel−parallel isomer **7**-d_1 cannot

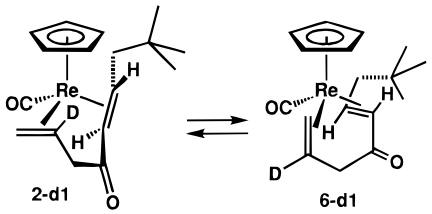

be excluded since such a process does not involve net hydrogen migration.

Isomerization via a C−H σ−Bond Complex. There are three ways that isomerization of allyl vinyl ketone complexes might occur without the intervention of a coordinatively unsaturated trappable intermediate. The first involves coordination of the ketone carbonyl to rhenium in place of an alkene ligand. A similar "conducted tour" mechanism[9] has been proposed by Kegley in the enantioface inversion of molybdenum acrylate ester complexes.[10,11] Molybdenum was suggested to slide along the conjugated π-system to the ester carbonyl. This allows rotation of the uncomplexed alkene by 180° prior to recoordination to molybdenum, and accomplishes the enantioface inversion.

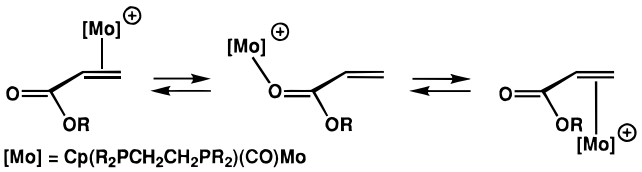

While it is easy to envision how a metal might glide down the π-system of Kegley's acrylate complexes, the constrained geometry of our chelated allyl vinyl ketone complexes makes such a process less likely. In the starting parallel−perpendicular complex **2**, rhenium migration from the vinyl double bond to the carbonyl π-system appears difficult because of the 130° dihedral angle between the two π-systems [C(6)−C(5)−C(4)−O(4)] and because the carbonyl oxygen is directed away from rhenium [Re−C(5)−C(4)−O(4) dihedral angle = 140°]. Similarly, the migration of Re from the allyl π-bond to a carbonyl of parallel−parallel intermediate such as **12-exo** appears difficult because this involves migration across a saturated carbon and because the planes of the allyl π-bond and the carbonyl π-bond are nearly orthogonal [the O(4)−C(4)−C(5)−Re dihedral angle is 156.7°].

Two closely related isomerization pathways that avoid coordinatively unsaturated intermediates involve either C−H "σ-bond" complexes as intermediates or reversible insertion into a C−H bond to give metal hydride intermediates. Gladysz' detailed studies of the enantioface inversion of rhenium alkene complexes such as $Cp(NO)(PPh_3)Re(styrene)^+$ effectively excluded all mechanisms except these two, but the data were consistent with either a C−H "σ-bond" complex or a fully inserted intermediate.[12,13] Based on isotope effect measure-

(7) Casey, C. P.; Underiner, T. L.; Vosejpka, P. C.; Gavney, J. A., Jr.; Kiprof, P. *J. Am. Chem. Soc.* **1992**, *114*, 10826−10834.

(8) Reduction of propargyl alcohol with $LiAlD_4$ gave $CH_2{=}CDCH_2$-OH, which was converted to $CH_2{=}CDCH_2Br$ by treatment with CBr_4 and Ph_3P. Grant, B.; Djerassi, C. *J. Org. Chem.* **1974**, *39*, 968. Molloy, B. B.; Hauser, K. L. *J. Chem. Soc., Chem. Commun.* **1968**, 1017. Hooz, J.; Gilani, S. S. H. *Can. J. Chem.* **1968**, *46*, 86.

(9) (a) Ford, W. T.; Cram, D. J. *J. Am. Chem. Soc.* **1968**, *90*, 2606, 2612. (b) Chu, K. C.; Cram, D. J. *J. Am. Chem. Soc.* **1972**, *94*, 3521.

(10) Kegley, S. E.; Bergstrom, D. T.; Crocker, L. S.; Weiss, E. P.; Berndt, W. G.; Rheingold, A. L. *Organometallics* **1991**, *10*, 567.

(11) Kegley, S. E.; Walter, K. A.; Bergstrom, D. T.; MacFarland, D. K.; Young, B. G.; Rheingold, A. L. *Organometallics* **1993**, *12*, 2339.

(12) (a) Peng, T.-S.; Gladysz, J. A. *J. Am. Chem. Soc.* **1992**, *114*, 4174. (b) Peng, T.-S.; Gladysz, J. A. *J. Chem. Soc., Chem. Commun.* **1990**, 902.

Scheme 7

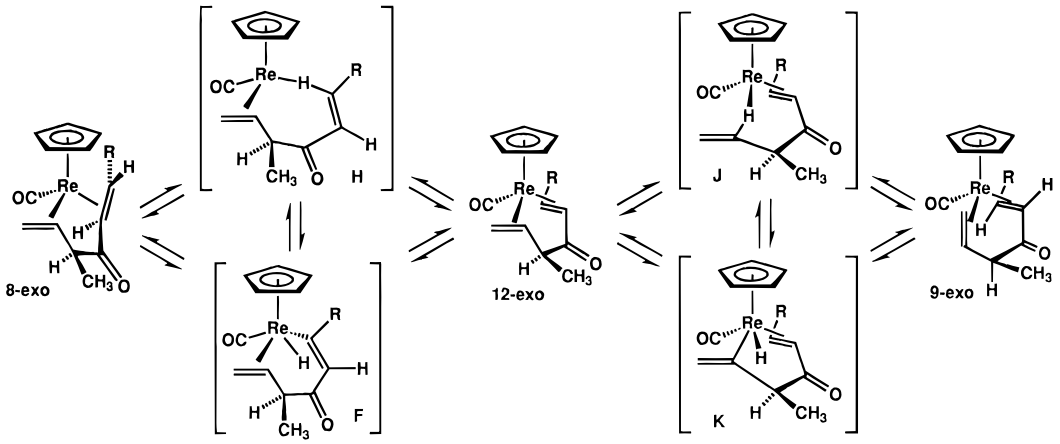

ments, Gladysz favored isomerization by a complex with an agostic interaction between Re and the C−H bond trans to the phenyl group. A larger isotope effect [k(H)/k(=CHD$_E$) = 1.64] was associated with the agostic C−H bond and smaller isotope effects were associated with the other hydrogens [k(H)/k(=CHD$_Z$) = 1.07, and k(H)/k(=CDPh) = 1.15], whose s-character increases somewhat upon decomplexation.

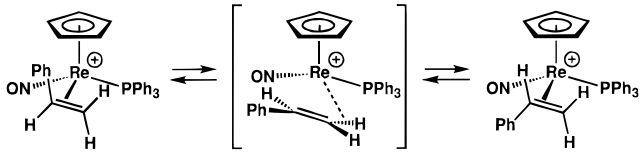

In the case of the isomerization of allyl vinyl ketone complex **8-exo**, we suggest that rhenium slides from the vinyl π-bond to the β-vinyl hydrogen to form the σ-C−H complex **H** that then collapses by rhenium migration to the opposite enantioface of the π-bond to give a parallel−parallel allyl vinyl ketone complex **12-exo** (Scheme 7). The second step in the isomerization then occurs via a similar process in which rhenium slides from the allyl π-bond to the secondary vinyl hydrogen to form the σ-C−H complex **J**, which then collapses by rhenium migration to the opposite enantioface to give **9-exo**. A mechanism involving complete insertion of rhenium into the C−H bond to give intermediates **F** and **K** cannot be excluded.

Two deuterated derivatives of **8-exo** were synthesized to examine isotope effects on the transformation of intermediate **12-exo** to **9-exo**. *exo*-Cp(CO)Re[η^2,η^2-CH$_2$=CDCH(CH$_3$)COCH=CHCH$_2$CMe$_3$] (**8-exo-d_1**) was prepared by reaction of K$^+$Cp(CO)$_2$Re[(*E*)-CH=CHCH$_2$-CMe$_3$]$^-$ (**11**) with *trans*-CH$_3$CH=CDCH$_2$Br[14] and was purified by preparative thin-layer chromatography.

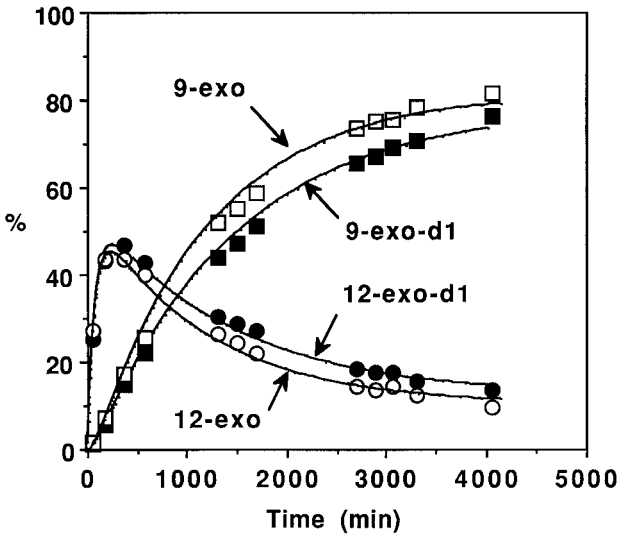

Figure 4. Isomerization of **8-exo** and **8-exo-d_1** at 99.8 °C. For clarity, only the intermediates **12-exo** (○) and **12-exo-d_1** (●) and final products **9-exo** (□) and **9-exo-d_1** (■) are shown.

exo-Cp(CO)Re[η^2,η^2-CD$_2$=CHCH(CH$_3$)COCH=CHCH$_2$-CMe$_3$] (**8-exo-d_2**) was prepared by reaction of K$^+$Cp-(CO)$_2$Re[(*E*)-CH=CHCH$_2$CMe$_3$]$^-$ (**11**) with *trans*-CH$_3$-CH=CHCD$_2$Br[15] and was purified by preparative thin-layer chromatography. Careful kinetic measurements on paired samples gave reliable kinetic plots. As expected, no isotope effect was seen on the rate of conversion of **8-exo** to the parallel−parallel intermediate **12-exo** since this transformation does not involve the deuterated π-bond. However, a small but significant isotope effect was observed for the conversion of deuterated **12-exo-d_1** to **9-exo-d_1** (Figure 4). The data were fit to a kinetic model for isomerization of **8-exo-d_1** to **12-exo-d_1** and **9-exo-d_1** using the program GEAR[6] with $k_{8\rightarrow12} = (1.20 \pm 0.02) \times 10^{-4}$ s^{-1}, $k_{12\rightarrow8} = (9.5 \pm 0.1) \times 10^{-5}$ s^{-1}, $k_{12\rightarrow9} = (1.73 \pm 0.03) \times 10^{-5}$ s^{-1}, and $k_{9\rightarrow12} = (2.2 \pm 0.1) \times 10^{-6}$ s^{-1}. This corresponds to an isotope effect of $k_H/k_D = 1.29 \pm 0.05$ for conversion of **12-exo-d_1** to **9-exo-d_1**. A smaller but measurable isotope effect was seen in the conversion of **8-exo-d_2** to **12-exo-d_2** and **9-exo-d_2** with $k_{8\rightarrow12} = (1.20 \pm 0.02) \times 10^{-4}$ s^{-1}, $k_{12\rightarrow8} =$

(13) For related papers, see: (a) Peng, T.-S.; Arif, A. M.; Gladysz, J. A. *Helvetica Chim. Acta* **1992**, *75*, 442. (b) Pu, J.; Peng, T.-S.; Arif, A. M.; Gladysz, J. A. *Organometallics* **1992**, *11*, 3232. (c) Wang, Y.; Agbossou, F.; Dalton, D. M.; Liu, Y.; Arif, A. M.; Gladysz, J. A. *Organometallics* **1993**, *12*, 2699. (d) Pu, J.; Peng, T.-S.; Mayne, C. L.; Arif, A. M.; Gladysz, J. A. *Organometallics* **1993**, *12*, 2686. (e) Peng, T.-S.; Wang, Y.; Arif, A. M.; Gladysz, J. A. *Organometallics* **1993**, *12*, 4535. (f) Peng, T.-S.; Pu, J.; Gladysz, J. A. *Organometallics* **1994**, *13*, 929. (g) Sanaú, M.; Peng, T.-S.; Arif, A. M.; Gladysz, J. A. *J. Organomet. Chem.* **1995**, *503*, 235.

(14) Reduction of CH$_3$C≡CCH$_2$OH with LiAlD4 gave *trans*-CH$_3$-CH=CDCH$_2$OH, which was converted to CH$_3$CH=CDCH$_2$Br by treatment with CBr$_4$ and Ph$_3$P. Grant, B.; Djerassi, C. *J. Org. Chem.* **1974**, *39*, 968. Molloy, B. B.; Hauser, K. L. *J. Chem. Soc., Chem. Commun.* **1968**, 1017. Hooz, J.; Gilani, S. S. H. *Can. J. Chem.* **1968**, *46*, 86.

(15) Reduction of *trans*-CH$_3$CH=CHCO$_2$Me with LiAlD4 gave *trans*-CH$_3$CH=CHCD$_2$OH which was converted to CH$_3$CH=CHCD$_2$Br by treatment with CBr$_4$ and Ph$_3$P. Orfanopoulos, M.; Smonou, I.; Foote, C. S. *J. Am. Chem. Soc.* **1990**, *112*, 3607. Hooz, J.; Gilani, S. S. H. *Can. J. Chem.* **1968**, *46*, 86.

$(9.5 \pm 0.1) \times 10^{-5}$ s^{-1}, $k_{12\rightarrow 9} = (1.88 \pm 0.03) \times 10^{-5}$ s^{-1}, and $k_{9\rightarrow 12} = (2.4 \pm 0.1) \times 10^{-6}$ s^{-1}. This corresponds to an isotope effect of $k_H/k_D = 1.19 \pm 0.05$ for conversion of **12-exo-*d*$_2$** to **9-exo-*d*$_2$**.

These isotope effects are similar in magnitude to those observed by Gladysz for $Cp(NO)(PPh_3)Re(styrene)^+$.[12] The larger magnitude of the isotope effect for **12-exo-*d*$_1$** than for **12-exo-*d*$_2$** is consistent with isomerization via the σ-C−H complex **J** in which rhenium interacts with a secondary vinyl hydrogen. Once again, however, complete insertion of rhenium into the C−H bond to give intermediate **K** cannot be excluded.

Conclusion. The allyl vinyl ketone complex **2** rearranges to diastereomer **6** without the formation of trappable, unsaturated intermediates. The reaction takes place with retention of stereochemistry at rhenium and with enantioface inversion of both complexed alkenes. The kinetically formed parallel−perpendicular isomer **2** rearranges by sequential enantioface inversion of the vinyl π-bond to give parallel−parallel intermediate **7** and then enantioface inversion of the allyl π-bond to form the perpendicular−parallel isomer **6**. No reversal to π-allyl or σ-allyl intermediates occurs in the isomerization. Enolization of allyl vinyl ketone complexes can occur but is not required in the isomerization. C−H insertion mechanisms that lead to net hydrogen migration were excluded by deuterium labeling studies. We propose a mechanism in which rhenium migrates to the opposite enantiofaces of the alkene ligands via σ-C−H complexes similar to those suggested by Gladysz.[12]

Experimental Section

General Information. ^{1}H NMR spectra were obtained on Bruker WP200, WP270, or AM500 spectrometers. $^{13}C\{^1H\}$ NMR spectra were obtained on a Bruker AM500 spectrometer (126 MHz). Infrared spectra were measured on a Mattson Polaris (FT) spectrometer. Mass spectra were determined on a Kratos MS-80. Elemental analyses were performed by Galbraith Laboratories, Inc. (Knoxville, TN).

Diethyl ether, hexane, and THF were distilled from purple solutions of sodium and benzophenone immediately prior to use. Dichloromethane, CD_2Cl_2, acetonitrile, and CD_3CN were dried over P_2O_5 or CaH_2 and distilled prior to use. CD_3OD (Aldrich) was used without further purification. Allyl bromide and 1-bromo-2-butene (Aldrich) were distilled prior to use. K^+-$Cp(CO)_2Re[(E)$-$CH{=}CHCH_2CMe_3]^-$ (**11**) and $C_5H_5(CO)Re(\eta^2,\eta^2$-$CH_2{=}CHCH_2COCH{=}CHCH_2CMe_3)$ (**2**) were prepared as previously reported.[1] Air-sensitive materials were manipulated in an inert atmosphere glovebox or by standard Schlenk techniques. Thermolysis reactions in acetonitrile at 100 °C (~2 atm) were carried out in sealed thick-walled NMR tubes or in thick-walled glass tubes equipped with extended-tip Teflon valves.

Equilibration of Isomers 2, 6, and 7 of $C_5H_5(CO)Re(\eta^2,\eta^2$-$CH_2{=}CHCH_2COCH{=}CHCH_2CMe_3)$. A 0.026 M CD_3CN solution of **2** was heated at 99.8 °C and monitored by ^{1}H NMR spectroscopy. The ratio of isomers was estimated by integration of the well-resolved Cp resonances of **2** (δ 4.99), **7** (δ 5.18), and **6** (δ 5.11). During the course of the equilibration, resonances assigned to the parallel−parallel isomer **7** were observed at δ 5.18 (s, Cp), 4.41 (d, J = 9.0 Hz, COC*H*=CH), 3.27 (ddd, J = 9.0, 6.6, 2.0 Hz, COCH=C*H*), and 0.97 (s, CMe_3). The percentage of **7** reached a maximum of ~8% during the first 2 h and then slowly decreased to an equilibrium value of ~4%. After 6 days, the ratio of **2:7:6** was 31:4:65 and showed no further change. Analysis of these kinetic data using the GEAR[6] program gave the following rate constants: $k_{27} = (1.92 \pm 0.03) \times 10^{-5}$ s^{-1}, $k_{72} = (1.23 \pm 0.02) \times 10^{-4}$ s^{-1}, $k_{76} = (4.38 \pm 0.0) \times 10^{-5}$ s^{-1}, and $k_{67} = (2.9 \pm 0.1) \times 10^{-6}$ s^{-1}. These rate constants correspond to $t_{1/2}$ = 1.4 h for equilibration of **2** and **7**, $t_{1/2}$ = 27 h for equilibration of **2** and **6**, and an equilibrium ratio of **2**:**7**:**6** of 28:4:67.

A CD_3CN solution of **6** (0.02 mmol) was heated at 105 °C for 14 days. Integration of the well-resolved ^{1}H NMR Cp resonances of **2**, **7**, and **6** showed a 62:4:34 equilibrium mixture, respectively.

Thermolysis of 2 in the Presence of PMe_3. When a CH_3CN solution of **2** [prepared from **11** [1] (10 mg, 0.023 mmol) and excess (0.45 mmol) allyl bromide in CH_3CN] and PMe_3 (0.044 mmol) was heated at 85 °C for 35 days, ^{1}H NMR analysis showed slow formation of **6** and resonances due to **2** and PMe_3 (δ 0.96, d, J = 2.0 Hz). No new doublets assignable to a coordinated PMe_3 ligand were observed. Cp resonances other than those of **2** and **6** comprised less than 10% of the total integration of all Cp resonances.

Thermolysis of 6 under ^{13}CO. When a CD_3CN solution of **6** (0.02 mmol) was sealed in an NMR tube under 0.8 atm of ^{13}CO and heated at 100 °C for 39 days, ^{1}H NMR analysis revealed formation of a 64:36 mixture of **6/2**. In the $^{13}C\{^1H\}$ NMR spectrum, no increase in the relative intensities of the carbonyl resonances of **6** (δ 212.1, 206.3) or of **2** (δ 212.8, 208.2) compared with the Cp resonances of **2** and **6** was observed.

Thermolysis of 2 in the Presence of CD_3OD. After 2 weeks at room temperature, a solution of **2** in 4:1 CD_3CN/CD_3OD showed no decrease in the intensity of any ^{1}H NMR resonances of **2** or simplification of any multiplet. When the solution was heated at 105 °C for 1 week, formation of a 1:1.1 ratio of **2/6** was observed by ^{1}H NMR spectroscopy. Separation of the isomers by TLC (silica gel, 1:1 hexane/Et_2O) allowed assignment of the position of deuterium incorporation in both **2** and **6**. For **2**, the ^{1}H NMR resonances of the allylic protons α to the ketone carbonyl at δ 2.00 and 1.66 were diminished (0.3 H) relative to a signal at δ 3.38 (1 H). For **6**, the ^{1}H NMR resonances of the allylic protons α- to the ketone carbonyl at δ 2.09 and 1.99 were greatly diminished (0.03 H) and the central allylic proton resonance at δ 2.42 (dd, J = 9.8, 7.3 Hz) was coupled to one fewer protons than undeuterated **6** (ddd, J = 9.8, 7.3, 6.4 Hz).

When a solution of **2** in 4:1 CD_3CN/CD_3OD was heated at 100 °C for 69 h, partial equilibration to a 2:1 mixture of **2**/**6** occurred. The mixture was halfway to equilibrium. ^{1}H NMR analysis of samples of **2** and **6** isolated by preparative TLC showed ~1.4 deuterium atoms/molecule for both **2** and **6**. Mass spectral analysis of the molecular ion cluster (M^+ *m*/*e* 446) of **2** showed 17% d_0, 42% d_1, and 41% d_2. Similar analysis of **6** showed 10% d_0, 74% d_1, and 17% d_2.

***endo*- and *exo*-$C_5H_5(CO)Re[\eta^2,\eta^2$-$CH_2{=}CHCH(CH_3)$-$COCH{=}CHCH_2CMe_3]$ (8-endo and 8-exo).** When a yellow THF solution of **11** [1] (108 mg, 0.25 mmol) and excess crotyl bromide (0.94 mmol) was warmed from −78 °C to room temperature, a white precipitate (KBr) formed and the color darkened to orange. After 10 min, volatile materials were removed under vacuum and CH_3CN was condensed onto the residue. The resulting suspension was stirred overnight, solvent was evaporated, and the residue was thin-layer chromatographed (silica gel, 1:1 hexane/Et_2O) to give a yellow band (R_f = 0.4) from which **8-endo** was isolated as a yellow oil (20 mg, 17%), and a broad pale yellow band (R_f = 0.15) from which **8**-exo was isolated as a yellow oil (80 mg, 70%).

For **8-endo**: ^{1}H NMR (270 MHz, CD_2Cl_2) δ 4.91 (s, C_5H_5), 3.36 (ddd, J = 10.2, 8.1, 2.3 Hz, COCH=C*H*), 2.59 (d, J = 8.6 Hz, COC*H*=CH), 2.31 (ddd, J = 10.2, 8.1, 6.6 Hz, CH_2=C*H*), 1.95 (dd, J = 12.9, 2.3 Hz, C*H*HCMe$_3$), 1.92 (pentet, J = 6.6 Hz, C*H*CH_3), 1.90 (dd, J = 8.1, 3.3 Hz, C*H*H=CH), 1.48 (dd, J = 10.2, 3.3 Hz, CH*H*=CH), 1.06 (d, J = 6.6 Hz, CH_3), 0.90 (s, CMe_3), 0.70 (dd, J = 12.9, 10.2 Hz, CH*H*CMe$_3$); $^{13}C\{^1H\}$ NMR (126 MHz, CD_3CN) δ 213.2, 210.1 (COs), 85.5 (C_5H_5), 73.0 (*C*H=CHCO), 57.6 (CH_2CMe_3), 41.6, 35.6 (CO*C*H=CH and *C*HCH_3), 35.3 (*C*Me$_3$), 29.5 (C*Me*$_3$), 21.3 (CH_2=*C*H), 16.7 (CH_3),

10.2 (*C*H2=CH); IR (CH_2Cl_2) 1923 (s), 1677 (m) cm^{-1}; HRMS calcd for $C_{18}H_{25}O_2Re$ 460.1412, found 460.1436. Anal. Calcd for $C_{18}H_{25}O_2Re$: C, 47.04; H, 5.48. Found, C, 47.21; H, 5.58.

Single crystals of **8-endo** suitable for X-ray structural analysis were obtained by cooling a concentrated CD_3CN solution of **8-endo** in a 5 mm tube to −15 °C. Complete crystallographic data, atomic coordinates, and refinement data are given in Supporting Information.

For **8-exo**: ^1H NMR (270 MHz, CD_2Cl_2) δ 4.98 (s, C_5H_5), 3.90 (ddd, J = 11.0, 8.7, 2.2 Hz, COCH=C*H*), 2.76 (dd, J = 7.5, 2.5 Hz, C*H*H=CH), 2.56 (br d, J = 9.0 Hz, COC*H*=CH), 2.51 (ddd, J = 9.5, 7.5, 4.6 Hz, CH_2=C*H*), 2.45 (qd, J = 7.0, 4.6 Hz, C*H*CH_3), 2.20 (dd, J = 9.5, 2.5 Hz, CH*H*=CH), 2.07 (dd, J = 13.0, 2.2 Hz, C*H*HCMe$_3$), 1.20 (d, J = 7.0 Hz, CH_3), 0.96 (dd, J = 12.9, 10.5 Hz, CH*H*CMe$_3$) 0.92 (s, CMe$_3$); ^{13}C {^1H} NMR (126 MHz, CD_3CN) δ 206.4, 197.5 (COs); 87.3 (C_5H_5), 70.2 (COCH=*C*H), 56.8 (CH_2CMe_3), 43.4, 41.8 (CH_2=*C*H and CO*C*H=CH), 34.9 (*C*Me$_3$), 29.8 (*C*HCH_3), 29.5 (C*Me*$_3$), 26.4 (CH_2=CH), 15.8 (CH_3), IR (CH_2Cl_2) 1895 (s), 1664 (m) cm^{-1}; HRMS calcd for $C_{18}H_{25}O_2Re$ 460.1412, found 460.1416. Anal. Calcd for $C_{18}H_{25}O_2Re$: C, 47.04; H, 5.48. Found: C, 46.61; H, 5.12.

Single crystals of **8-exo** suitable for X-ray structural analysis were obtained by slow evaporation of a diisopropyl ether solution of **8-exo** at −15 °C. Complete crystallographic data, atomic coordinates, and refinement data are given in Supporting Information.

***exo*-$C_5H_5(CO)Re[\eta^2,\eta^2$-$CH_2$=CHCH($CH_3$)COCH=$CHCH_2$-CMe$_3$] (9-exo) from Thermolysis of 8-exo.** A CD_3CN solution of **8**-exo (75 mg, 0.16 mmol) was heated at 100 °C in a sealed NMR tube. After 5 days, ^1H NMR analysis showed 72% **9-exo** (δ 5.10), 10% **12-exo** (δ 5.21), 8% **8-exo** (δ 5.03), and two minor Cp resonances at δ 5.14 (5%) and 4.98 (5%). Pure **9**-exo (20 mg, 44%) was obtained by TLC (silica gel, hexane/Et_2O 2/1, R_f = 0.07) followed by recrystallization from cold CH_3CN. For **9**-exo, ^1H NMR (270 MHz, CD_2Cl_2) δ 5.08 (s, C_5H_5), 3.28 (ddd, J = 11.1, 9.0, 2.2 Hz, COCH=C*H*), 2.65 (d, J = 9.0 Hz, COC*H*=CH), 2.6 (m, 2H, C*H*H=C*H*), 2.11 (dd, J = 13.4, 2.2 Hz, C*H*HCMe$_3$), 1.96 (pentet, J = 6.7 Hz, C*H*CH_3), 1.77 (d, J = 8.6 Hz, CH*H*=CH), 1.11 (d, J = 6.7 Hz, CH_3), 0.95 (s, CMe$_3$), 0.85 (dd, J = 13.4, 11.1 Hz, CH*H*CMe$_3$); ^{13}C {^1H} NMR (126 MHz, CD_3CN) δ 212.9, 207.8 (COs), 84.8 (C_5H_5), 55.1 (CH_2CMe_3), 54.2, 48.8 (COCH=*C*H and *C*HCH$_3$), 39.4 (CH_2=*C*H), 35.0 (CO*C*H=CH), 34.1 (*C*Me$_3$), 29.5 (C*Me*$_3$), 19.2 (CH_2=CH), 17.0 (CH_3), IR (CH_2Cl_2) 1921 (s), 1661 (m) cm^{-1}; HRMS calcd for $C_{18}H_{25}O_2Re$ 460.1412, found 460.1380. Anal. Calcd for $C_{18}H_{25}O_2Re$: C, 47.04; H, 5.48. Found: C, 47.36; H, 5.22.

Single crystals of **9-exo** were obtained by cooling a concentrated CD_3CN solution of **9-exo** to −15 °C. Complete crystallographic data, atomic coordinates, and refinement data are given in Supporting Information.

$C_5H_5(CO)Re[\eta^2,\eta^2$-$CH_2$=CHCH($CH_3$)COCH=$CHCH_2$C-Me$_3$] (12-exo) from Thermolysis of 8-exo. When a CD_3CN solution of **8-exo** was heated at 100 ± 3 °C for 2 h, ^1H NMR analysis showed a 1.2:1 ratio of Cp resonances for starting material **8-exo** (δ 5.03)/**12-exo** (δ 5.21), and a small amount of rearranged isomer **9-exo** (δ 5.10). Preparative TLC (silica gel, 1:1 hexane/Et_2O) gave a faster moving yellow band (R_f = 0.4) from which **12-exo** was isolated as a yellow oil. For **12-exo**, ^1H NMR (CD_2Cl_2, 500 MHz): δ 5.16 (s, Cp), 4.29 (d, J = 9.6 Hz, COC*H*=CH), 2.80 (CH=C*H*H), 2.32 (dd, J = 13.3, 2.3 Hz, C*H*HCMe$_3$), 2.29 (ddd, J = 11.6, 9.5, 2.3 Hz, COCH=C*H*), 1.84 (td, J = 9.8, 7.8 Hz, C*H*=CH_2), 1.20 (dd, J = 10.1, 2.5 Hz, CH=CH*H*), 1.10 (d, J = 6.7 Hz, CH_3), 1.06 (dd, J = 13.4, 11.7 Hz, CH*H*CMe$_3$), 0.95 (s, CMe$_3$), 0.57 (dq, J = 9.5, 6.7 Hz, C*H*CH_3); ^{13}C {^1H} NMR (126 MHz, CD_2Cl_2) COs were not observed, δ 87.1 (Cp), 59.0, 55.7, 50.6, 43.9, 34.3 (*C*Me$_3$), 29.4 (C*Me*$_3$), 23.0, 19.1, 18.2; IR (CH_2Cl_2) 1892 (vs), 1685 (s) cm^{-1}; HRMS calcd for $C_{18}H_{25}O_2Re$ 460.1412, found 460.1388. Anal. Calcd for $C_{18}H_{25}O_2Re$: C, 47.04; H, 5.48. Found: C, 46.89; H, 5.14.

Single crystals of **12-exo** were obtained by cooling a concentrated CD_3CN solution of **9-exo** to −20 °C. Complete crystallographic data, atomic coordinates, and refinement data are given in Supporting Information.

Thermolysis of 8-exo in the Presence of CD_3OD. When a solution of **8-exo** in 4:1 CD_3CN/CD_3OD was heated at 100 °C and monitored after 5, 15, and 24 h, ^1H NMR spectroscopy showed the formation of **12-exo** (δ 5.20) and **9-exo** (δ 5.10). The observation of a methyl doublet for **8-exo** at δ 1.17 (J = 6.9 Hz) and for **9-exo** at δ 1.04 (J = 6.7 Hz) demonstrated that no incorporation of deuterium had occurred. Incorporation of deuterium would have resulted in growth of a broad singlet at δ 1.17 (**8-exo**) or δ 1.04 (**9-exo**).

Thermolysis of 8-endo. When a CD_3CN solution of **8-endo** was heated at 100 °C for 13 days, a 25% decrease of **8-endo** (δ 4.91) was observed, along with growth of new Cp resonances at δ 5.15 (5%), 5.14 (10%), and 5.10 (**9-exo**, 10%). Due to the small quantities of new complexes formed, no attempt was made to isolate any rearranged products.

Thermolysis of 8-endo in the Presence of CD_3OD. When a solution of **8-endo** in 4:1 CD_3CN/CD_3OD was heated at 100 °C for 60 h, the ^1H NMR resonance of the α-methyl group at δ 1.01 was an unchanged doublet (J = 6.5 Hz). Incorporation of deuterium from CD_3OD would have resulted in growth of a broad singlet at δ 1.01.

$C_5H_5(CO)Re(\eta^2,\eta^2$-$CH_2$=CHC($CH_3$)$_2$COCH=$CHCH_2$C-Me$_3$) (13). A solution of **11** (18 mg, 0.041 mmol) and excess 4-bromo-2-methyl-2-butene (0.41 mmol) in CH_3CN (2 mL) was stirred for 0.2 h at room temperature to give crude **13**. Solvent and excess 4-bromo-2-methyl-2-butene were evaporated under vacuum, and the residue was redissolved in CH_3CN (3 mL) and stirred for 15 h. Solvent was evaporated under vacuum, and the yellow oily residue was separated by flash chromatography (silica gel, CH_2Cl_2). A yellow oil (R_f = 0.19) was collected (19 mg, 99%): ^1H NMR (200 MHz, CD_3CN) δ 5.00 (s, C_5H_5), 3.58 (ddd, J = 11.2, 9.0, 2.2 Hz, COCH=C*H*), 2.57 (d, J = 9.0 Hz, COC*H*=CH), 2.52 (dd, J = 10.5, 8.5 Hz, C*H*=CH_2), 2.18 (dd, J = 8.5, 3.1 Hz, CH=C*H*H), 2.01 (dd, J = 13.5, 2.2 Hz, COCH=CHC*H*H), 1.79 (dd, J = 10.5, 3.1 Hz, CH=CH*H*), 1.04, 0.97 (singlets, diastereotopic CH_3's), 0.88 (s, CMe$_3$), 0.63 (dd, J = 13.4, 10.5 Hz, COCH=CHCH*H*); ^{13}C NMR (126 MHz, CD_3CN) δ 211.7 (s), 210.3 (s) (ReCO, RCOR′), 86.2 (d, J = 178 Hz, C_5H_5), 74.6 (d, J = 160 Hz), 58.8 (t, J = 127 Hz, *C*H_2-CMe$_3$), 43.5 (s, *C*Me$_2$), 42.2 (d, J = 150 Hz, CO*C*H=CH), 37.1 (d, J = 159 Hz, *C*H=CH_2), 35.4 (s, *C*Me$_3$), 29.7 (q, J = 127 Hz, C(*C*H_3)$_3$), 29.3 (q, J = 132 Hz), 26.2 (q, J = 132 Hz) (diastereotopic CH_3's), 16.4 (t, J = 155 Hz, CH=*C*H2); IR (CH_2Cl_2) 1920 (s), 1670 (m) cm^{-1}; HRMS calcd for $C_{19}H_{27}ReO_2$ 474.1569, found 474.1573.

Thermolysis of $C_5H_5(CO)Re(\eta^2,\eta^2$-$CH_2$=CHC($CH_3$)$_2$-COCH=$CHCH_2CMe_3$) (13). A sealed NMR tube containing a CD_3CN solution of **13** (12 mg, 0.025 mmol) was heated at 100 °C. After 3 h, ^1H NMR analysis of the Cp region showed 72% of the starting complex **13** remained (δ 5.00) and 28% of a new compound **14** (δ 5.15) was present. After 21 h at 100 °C, 65% **13** (δ 5.00), 32% **14** (δ 5.15), and 3% of a third compound **15** (δ 5.14) were observed. After 180 h, ^1H NMR analysis revealed an equilibrium mixture of 50% **13**, 28% **14**, and 22% **15**. Pure **14** (3.2 mg, 27%) was obtained by preparative TLC (silica gel, first development with 60:40 hexane/Et_2O; second development with 50:50 hexane/Et_2O, R_f = 0.44). Isomer **15** (2.3 mg, 20%) was separated from the starting complex by preparative TLC (silica gel, two elutions with CH_2Cl_2, R_f = 0.17).

For parallel−parallel isomer **14:** ^1H NMR (270 MHz, CD_3CN) δ 5.15 (s, Cp), 4.58 (d, J = 9.3 Hz, COC*H*=CH), 3.00 (dd, J = 8.3, 3.6 Hz, CH=C*H*H), 2.74 (dd, J = 11.0, 8.3 Hz, C*H*=CH_2), 2.65 (ddd, J = 9.3, 6.8, 2.5 Hz, COCH=C*H*), 2.06 (dd, J = 12.8, 2.6 Hz, CH*H*CMe$_3$), 1.22 (dd, J = 12.8, 6.8 Hz, C*H*HCMe$_3$), 1.34 (s, CH_3), 1.13 (dd, J = 11.0, 3.6 Hz, CH=CH*H*), 1.00 (s, CMe$_3$), 0.97 (s, CH_3); IR (CH_2Cl_2) 1895 (s), 1660 (m) cm^{-1}; HRMS calcd for $C_{19}H_{27}O_2Re$ 472.1541, found 472.1534.

Table 2. Crystal Structure Data for 8-exo, 8-endo, 9-exo, and 12-exo

	8-exo	**8**-endo	**9**-exo	**12**-exo
empirical formula	$C_{18}H_{25}O_2Re$	$C_{18}H_{25}O_2Re$	$C_{18}H_{25}O_2Re$	$C_{18}H_{25}O_2Re$
color, habit	yellow plate	yellow plate	yellow plate	yellow block
crystal size, mm	0.5 × 0.3 × 0.1	0.5 × 0.3 × 0.1	0.5 × 0.3 × 0.1	0.5 × 0.2 × 0.2
cryst syst	monoclinic	orthorhombic	triclinic	triclinic
space group	$P2_1/c$	*Pbca*	$P\bar{1}$	$P\bar{1}$
unit cell dimens				
a, Å	10.059(2)	15.695(7)	9.078(3)	8.926(2)
b, Å	15.081(3)	11.432(5)	9.541(4)	9.096(2)
c, Å	12.126(2)	18.785(7)	11.694(4)	11.467(2)
α, deg	90	90	66.33(3)	101.19(2)
β, deg	110.32(3)	90	83.74(2)	94.48(2)
γ, deg	90	90	64.14(3)	109.31(2)
vol, Å^3	1725.0(6)	3370(2)	832.1(5)	851.7(3)
no. of peaks to determine cell	17	25	25	25
θ range of cell peaks	6.0−11.5	12.5−15.0	13.5−15.0	12.5−15.0
temperature, K	113(2)	113(2)	113(2)	223(2)
Z	4	8	2	2
formula wt	459.58	459.58	459.58	459.58
density (calcd), Mg m^{-3}	1.770	1.811	1.834	1.792
abs coeff, mm^{-1}	7.046	7.213	7.304	7.136
F(000)	896	1792	448	448
R1, %	5.29	4.27	2.02	1.63
wR2, %	13.03	12.52	5.16	4.26
S, gof	1.054	1.414	1.139	1.131

For perpendicular−parallel isomer **15**: ^{1}H NMR (200 MHz, CD_3CN) *δ* 5.14 (s, Cp), 3.54 (ddd, *J* = 9.4, 7.2, 2.2 Hz, COCH=C*H*) 3.07 (d, *J* = 9.4 Hz, COC*H*=CH), 2.77 (dd, *J* = 7.7, 1.4 CH=C*H*H), 2.22 (dd, *J* = 10.3, 7.6 Hz, C*H*=CH_2), 2.12 (dd, *J* = 13.3, 2.2 Hz, CH*H*CMe_3), 2.08 (dd, *J* = 10.3, 1.4 Hz, CH=CH*H*), 1.09 (s, CH_3), 0.96 (s, CMe_3), 0.93 (s, CH_3), 0.86 (dd, *J* = 13.3, 7.2 Hz, C*H*HCMe_3); IR (CH_2Cl_2) 1914 (s), 1732 (m) cm^{-1}; HRMS calcd for $C_{19}H_{27}O_2Re$ 472.1541, found 472.1526.

Kinetic Isotope Effect Study. Aliquots (0.45 mL) of freshly prepared solutions of **8-exo**, **8-exo-*d*$_2$**, and **8-exo-*d*$_1$** (28.4 mg, 0.082 mmol, in 2.00 mL CD_3CN containing 7.3 *μ*L of C_6H_6 as an internal standard, 3.08 × 10^{-2} M) were placed in NMR tubes and degassed by three freeze−pump−thaw cycles. The tubes were flame-sealed and stored in a −10 °C freezer until used. Two different isotopic samples of **8** were totally immersed in a 99.8 ± 0.2 °C constant-temperature oil bath. At 2−4 h intervals, the tubes were withdrawn, washed with hexane and placed in an ice/water bath. Progress of the reaction was monitored by integration of the Cp resonances at *δ* 5.26, *δ* 5.13, and *δ* 5.01, and the total area was compared with the residual C_6H_6 signal.

X−ray Crystallographic Determination and Refinement of 8-exo, 8-endo, 9-exo, and 12-exo. Intensity data were obtained with graphite-monochromated Mo Kα radiation on Siemens P3f or P4 diffractometers at −160 or −50 °C (**12**-exo). Crystallographic computations were carried out with SHELXTL PLUS.[16] Empirical absorption corrections were applied only to the **9-exo** structure. Initial Re atom positions were obtained from interpretation of Patterson maps. Other non-hydrogen atoms were located from successive factor calculations and difference Fourier maps. All non-hydrogen atoms were refined anisotropically. Refinement of the **8-endo** structure required that restraints be applied to the displacement parameters. Hydrogen positions were initially determined from geometry and refined with a riding model by assuming U_{iso} to be 1.2 (1.4 for methyl groups) times the U_{eq} of the carrier atom. Tables of data collection parameters, least-squares refinement parameters, positional and thermal parameters, interatomic distances, bond angles, and idealized hydrogen atom positional parameters are available as Supporting Information.

Acknowledgment. Financial support from the National Science Foundation is gratefully acknowledged.

Supporting Information Available: X-ray crystallographic data for **8-exo**, **8-endo**, **9-exo**, and **12-exo** (40 pages). Ordering information is given on any current masthead page.

OM970004L

(16) Sheldrick, G. M. *SHELXTL PLUS Version 5 Reference Manual* Siemens Analytical X−Ray Instruments, 6300 Enterprise Drive, Madison, WI 53719, 1994.